

Africa–Eurasia kinematics control of long-wavelength tectonic deformation in the Central Mediterranean

A. M. Marotta and R. Sabadini

Geophysics Section, Department of Earth Sciences 'A. Desio', University of Milan, Italy. E-mail: anna.maria.marotta@unimi.it

Accepted 2008 July 1. Received 2008 May 15; in original form 2007 October 10

SUMMARY

We use a spherical thin sheet geophysical model to study the regional deformation pattern in the Central Mediterranean and compare model predictions with the deformation resulting from new ITRF2005 data, in terms of both amplitude and direction of the strain rate eigenvectors. We quantify the effects of the choice of a specific data set in defining the boundary conditions for Africa–Eurasia convergence in a predictive model that spreads the information resulting from a discrete data set over a continuum, such as the geodetic one. The fairly good agreement between geodetic and modelled patterns shows that, within the study area, the deformation predicted by tectonic models based on ITRF2005 boundary conditions (b.c.) for Africa–Eurasia relative motion differs from that predicted by models based on Deos2k b.c., only on long distances from the Africa–Eurasia boundary. Geodetically retrieved SSE–NNW compression and SSW–NNE extension are well reproduced by the eigenvectors of the strain-rate tensor in the central Mediterranean and Italian peninsula, with eigenvalues generally slightly underestimating the observed ones, resulting in a global strain-rate of the order of a few nanostrain yr^{-1} . The effects of viscosity contrasts across the model domain are assessed in terms of their impact on baseline variations and strain rates.

Key words: Intra-plate processes; Continental margins: convergent.

1 INTRODUCTION

Long GPS time-series, now available in the Mediterranean, make it possible to validate realistic finite element tectonic models in which deformation is driven by major plate tectonic processes such as Africa–Eurasia continental collision, by means of a systematic comparison between the predicted and the geodetic deformation, as deduced from recent ITRF solutions.

Recent studies based on ITRF2000 (Altamini *et al.* 2002), have already shown that the effects of the push from Africa is transmitted to Central Europe at the latitude of Potsdam, whereas postglacial rebound (PGR) is affecting GPS deformation patterns north of this site. Release of the new ITRF2005 solution (Altamini *et al.* 2007) allows us to focus on the GPS and modelled deformation style of the Central Mediterranean, a tectonically complex region including the Italian peninsula and the Tyrrhenian basin embedded between the African indenter and continental Europe. In this area, in fact, tectonics causes an enigmatic regional deformation pattern, characterized by areas subjected to extension, like the Tyrrhenian basin, within the context of active Africa–Eurasia convergence. To analyse the regional deformation field, we perform numerical models, based on the viscous thin sheet approximation, within the scheme implemented by Marotta *et al.* (2004), to study long wavelength deformation in central and Northern Europe. Model predictions, in terms of baseline rate of change and strain rate eigenvalues and eigenvectors, are compared with the geodetically

retrieved deformation, based on the most recent space geodesy velocity ITRF2005 solution.

A tectonic model for intracontinental deformation requires two major constituents to be correctly defined, which are the set of differential equations prescribing the conservation of linear momentum in the absence of inertial forces, as per long timescale processes, and the tectonic boundary conditions at the borders defining the geometry of the study region. The geophysical models developed in the last years (e.g. Jimenez-Munt *et al.* 2003; Marotta *et al.* 2004; Negrodo *et al.* 2004; Wang & Zheng-Ren 2006) are commonly constrained through boundary conditions based on NUVEL-1 or NUVEL-1A models (DeMets *et al.* 1994; DeMets & Dixon 1999). Recent works (among others, Sella *et al.* 2002; Fernandez *et al.* 2003; Nocquet & Calais 2003; Kremer *et al.* 2003), based on geodetic estimates of crustal velocities, pointed out that the global plate motion model NUVEL-1A is not consistent with the present day relative plate motion, and new models have been developed with particular attention to specific areas. REVEL-2000, a new model for recent plate motion of 19 plates, was developed by (Sella *et al.* 2002) and is based on space geodetic data, primarily GPS ones, from 1993 to 2000. According to REVEL-2000, about one third of the plate pairs shows significant differences between REVEL-2000 predictions and NUVEL-1A, with some plate pairs (Arabia–Eurasia, Arabia–Nubia, Eurasia–India) showing a slower movement with respect to that indicated by NUVEL-1A. Kremer *et al.* (2003), by solving for the velocity

gradient tensor field through the entire Earth surface, developed the global velocity model GSRM-1, based on GPS, VLBI and DORIS data, measured on rigid plates, as well as along plate boundaries. For the specific Africa–Eurasia relative motion, GSRM-1 predicts a lower rotation rate with respect to NUVEL-1A. Nocquet & Calais (2003) derived a new geodetic velocity field for Western Europe and Mediterranean by combining a selected set of ITRF2000 stations and three other regional networks (EUREF–EPN, RGP and REGAL). Their analysis shows an Africa–Eurasia convergence, 40–50 per cent slower than that indicated by NUVEL-1A, westerly rotated by 20° – 30° , confirming that NUVEL-1A is not accurate enough to describe the Africa–Eurasia convergence in western Mediterranean. However, they pointed out that more stations in the African plate and longer time-series would be necessary to derive a reliable kinematics between Africa and Eurasia, based on geodetic information. To overcome the poor data coverage of the African plate and to improve the Africa–Eurasia relative motion, Fernandez *et al.* (2003) developed a new model, Deos2k, based on ITRF2000 (Altamini *et al.* 2002) and new geodetic solutions obtained from six new GPS stations implemented in the Nubian region of the African plate and processed until the end of 2002. With respect to NUVEL-1A and the previous geodetic analysis, Deos2k improves the estimate of the Africa–Eurasia convergence, showing a slower convergence, more westerly oriented, with deviations of up to 20 per cent in azimuth and up to 40 per cent smaller in magnitude, whereas, west of the Gibraltar Strait, Deos2k and NUVEL-1A show similar trends.

By this work, we quantify the effects of the choice of a specific data set in defining the boundary conditions in a predictive model, which is used to spread over a continuum medium, both along the Earth surface and at depth, the information coming from a discrete data set, such as the geodetic one. Indeed, this aspect becomes crucial when models are used for strain and stress localization analysis in tectonically active regions. To this aim, we use the same methodological approach developed by Marotta *et al.* (2004). The observed geodetic deformation patterns will be discussed within the sole perspective of our comparative analysis between model predictions and observations and not for discussing differences among the various GPS solutions or reference frames.

2 GEODETIC DEFORMATION IN THE MEDITERRANEAN

The strain of the tectonically active area under study is obtained from ITRF2005 (Table 1).

We are interested in the differences among GPS velocities, from which it is possible to extract information on the strain of the area under study due to active tectonics. In particular, the deformation

Table 1. ITRF2005 GPS velocity solutions in the sites referred in the present analysis.

SITE	V_x (cm yr ⁻¹)	V_y (cm yr ⁻¹)	V_z (cm yr ⁻¹)
OBER	-1.48 ± 0.03	1.76 ± 0.01	1.14 ± 0.03
GENO	-1.4 ± 0.1	1.89 ± 0.03	1.16 ± 0.06
VENE	-1.65 ± 0.05	1.79 ± 0.02	1.24 ± 0.05
GRAZ	-1.67 ± 0.01	1.81 ± 0.01	1.07 ± 0.02
CAGL	-1.32 ± 0.02	1.97 ± 0.01	1.27 ± 0.02
MATE	-1.79 ± 0.01	1.88 ± 0.01	1.55 ± 0.01
LAMP	-1.5 ± 0.1	1.68 ± 0.06	1.53 ± 0.07
NOTO	-1.75 ± 0.01	1.72 ± 0.01	1.55 ± 0.01

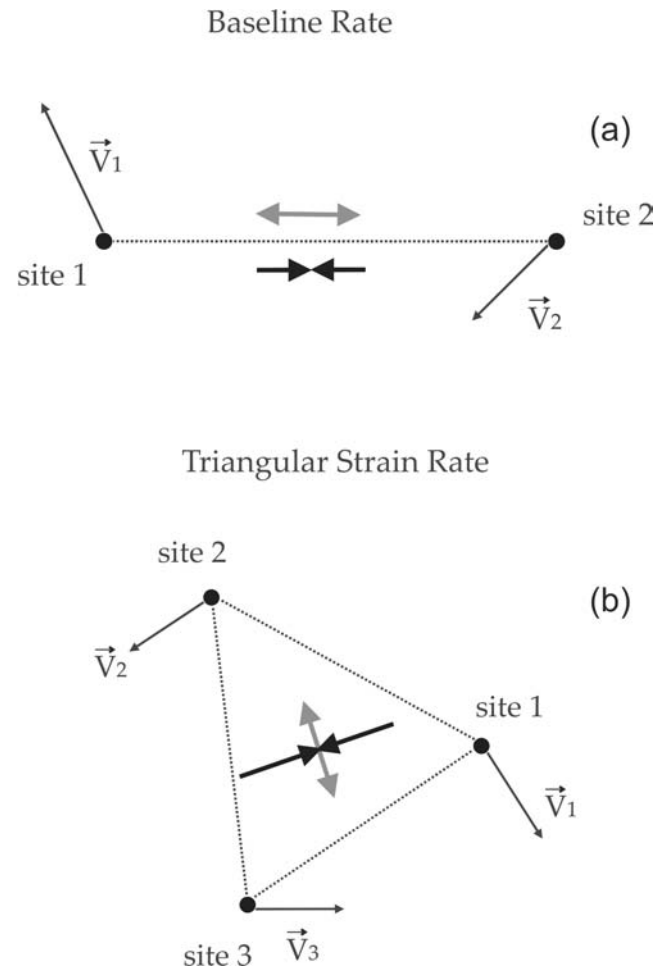


Figure 1. (a) Schematic representation of how baseline rate of change between two reference geodetic sites is calculated. Convergent black and divergent grey arrows indicate shortening and elongation, respectively. (b) Schematic representation of how triangular strain rate in a triangular area, delimited by three reference geodetic sites, is calculated. Convergent black and divergent grey arrows indicate compression and extensional strain rate eigenvectors, respectively.

pattern is analysed in terms of baseline rate of change between two GPS sites and strain rates within triangular domains. The baseline rate of change, now on baseline rate, is obtained by projecting the relative velocities between two geodetic sites along the line connecting them and represents the rate of shortening or of elongation of the corresponding baseline, as shown in Fig. 1. By triangular strain rate we mean the quantities related to the strain rate tensor evaluated in triangular areas defined by three geodetic sites where velocity is known, i.e. its eigenvalues and eigenvectors, as shown in Fig. 1. Baselines and triangular domains are chosen so as to be representative of global deformation of characteristic tectonic units like the Tyrrhenian and of changing distances between key GPS sites like MATE with respect to CAGL, which is indicative of the effects of the African indenter on the Adriatic microplate, contouring to the East the Tyrrhenian domain.

Fig. 2, based on ITRF2005, shows the geodetic baseline rate of change calculated along generally trending SE–NW and E–W baselines to elucidate the compression due to Africa–Eurasia convergence, which is in fact visible in the SE–NW shortening, and the extension between Sardinia and Adriatic GPS sites as MATE and VENE. Yellow indicates shortening and cyan elongation, with

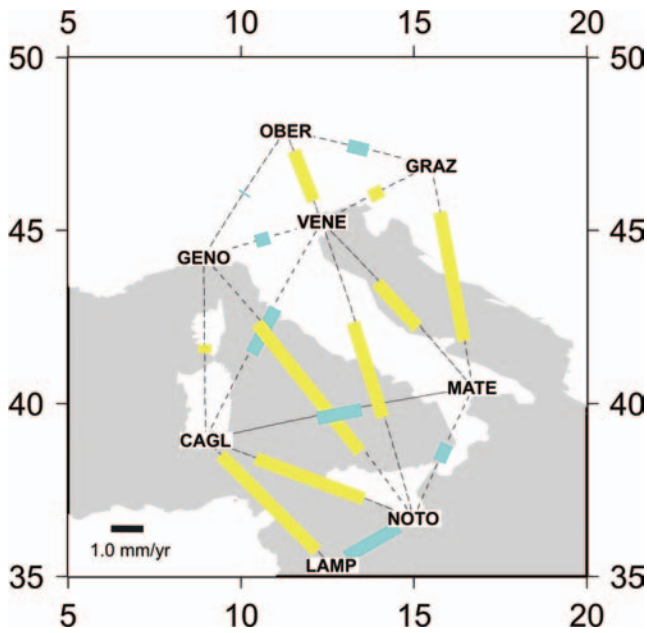


Figure 2. Geodetic baseline rates of change, calculated along SE–NW and E–W generally trending baselines in the Tyrrhenian area and based on GPS ITRF2005 solutions. Yellow indicates shortening and cyan elongation, with the length of the bars proportional to the magnitude of the baseline rates, in mm yr^{-1} .

Table 2. Observed baseline rates of change as deduced from ITRF2005 GPS velocity solutions.

BASELINE	RATE OF CHANGE (mm yr^{-1})
LAMP–CAGL	-4.2 ± 0.3
LAMP–NOTO	1.9 ± 0.3
NOTO–CAGL	-3.6 ± 0.1
NOTO–MATE	0.58 ± 0.02
MATE–CAGL	1.4 ± 0.1
MATE–VENE	-1.9 ± 0.1
VENE–CAGL	1.6 ± 0.1
VENE–GENO	0.4 ± 0.1
GENO–CAGL	-0.26 ± 0.05
VENE–OBER	-1.7 ± 0.1
OBER–GENO	0.1 ± 0.1
VENE–NOTO	-3.04 ± 0.03
NOTO–GENO	-5.1 ± 0.1
GRAZ–VENE	-0.4 ± 0.1
GRAZ–OBER	0.6 ± 0.1
GRAZ–MATE	-4.03 ± 0.02

the length of the bars proportional to the magnitude of the baseline rates, in mm yr^{-1} . ITRF2005 solution supports compression along the S–N directed baselines and extension along the E–W directed ones. The specific values are listed in Table 2, with the corresponding errors. A notable feature is that the ITRF2005 solution reveals an intense S–N shortening in the Tyrrhenian area, as evidenced by the -5.1 mm yr^{-1} shortening GENO–NOTO in the Central Tyrrhenian. This large shortening is accompanied by a small extension in the E–W direction, of about 1.4 mm yr^{-1} along the Adriatic site MATE and CAGL.

Similar considerations hold when the 2-D deformation pattern is analysed. Fig. 3 shows the eigenvectors of strain rates calculated

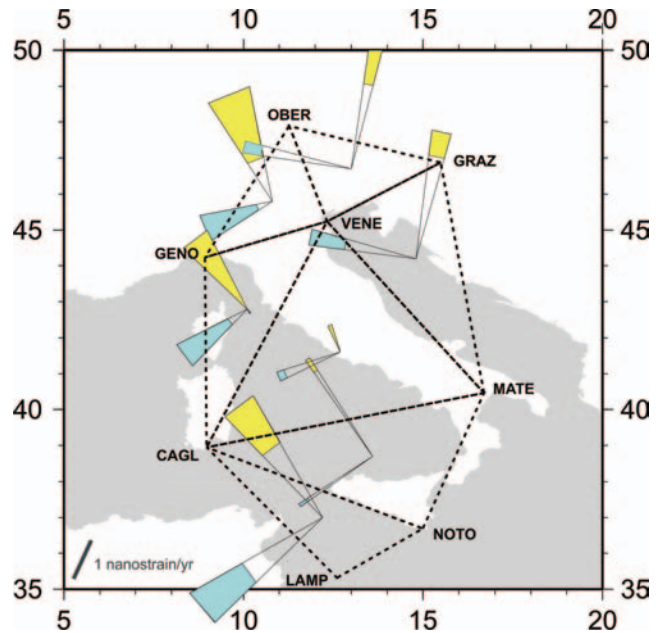


Figure 3. Eigenvectors of strain rates, calculated over triangular domain in the Tyrrhenian area, based on GPS ITRF2005 solutions. Yellow indicates compression and cyan extension, with the size of the circular sectors proportional to the magnitude of the eigenvector magnitude and azimuth uncertainties, in $\text{nanostrain yr}^{-1}$.

Table 3. Observed strain rates as deduced from ITRF2005 GPS velocity solutions.

TRIANGLE	Eigenvalue ϵ_1 $\text{nanostrain yr}^{-1}$	Eigenvalue ϵ_2 $\text{nanostrain yr}^{-1}$	Azimuth of ϵ_2 degree
LAMP–NOTO–CAGL	7.6 ± 2.6	-6.3 ± 1.5	-36.9 ± 7.3
NOTO–MATE–CAGL	4.6 ± 0.3	-6.1 ± 0.4	-33.8 ± 1.2
MATE–VENE–CAGL	3.5 ± 0.2	-0.8 ± 0.8	-21.7 ± 4.3
GRAZ–OBER–VENE	5.0 ± 1.0	-6.5 ± 0.7	11.5 ± 4.3
GRAZ–OBER–VENE	5.6 ± 0.5	-6.9 ± 2.1	11.5 ± 3.2
VENE–GENO–CAGL	2.8 ± 1.6	-2.3 ± 2.6	-36.6 ± 9.7
OBER–GENO–VENE	2.5 ± 1.6	-4.5 ± 2.0	-22.2 ± 10.9

over triangular areas. The specific values are listed in Table 3, with the corresponding errors.

In the center of Mediterranean ITRF2005 indicates a peculiar regional scale 2-D deformation pattern characterized by SSE–NNW directed compression (yellow colour) and the SW–NE directed extension (cyan colour). A clockwise rotation of the strain eigenvectors occurs, instead, inside the triangles extending from the Adriatic to the east. This new deformation style, with compression occurring along the SSW–NNE direction and extension along the NW–SE direction, persists at high latitudes, beside the Alpine front (Fig. 4), as shown in Marotta & Sabadini (2004) and Marotta (2005).

3 GEOPHYSICAL MODELLING OF TECTONIC DEFORMATION

The constituent of our tectonic model, represented by the solver of the differential equations implemented by Marotta *et al.* (2004), is based on a spherical thin sheet approximation within a finite element scheme. An incompressible, viscous model is adopted, which treats the lithosphere as a stratified viscous sheet, with

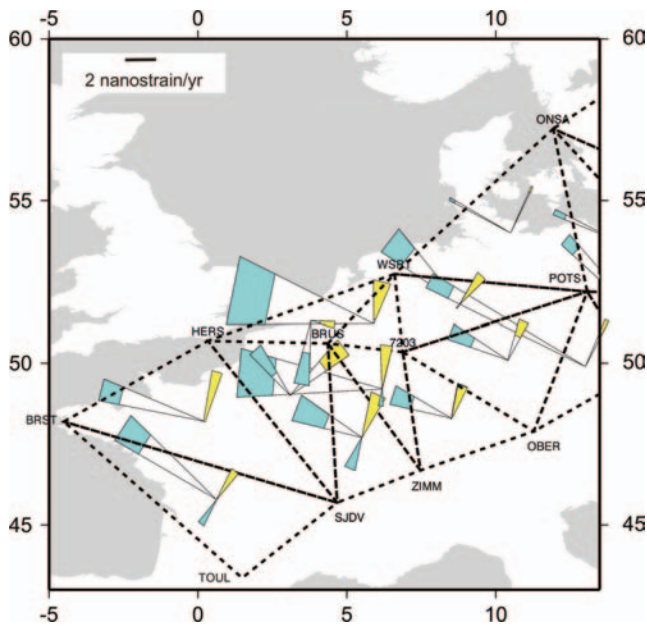


Figure 4. Eigenvectors of strain rates, calculated over triangular domain in Central Europe and based on GPS ITRF2005 solutions. Yellow indicates compression and cyan extension, with the size of the circular sectors proportional to the magnitude of the eigenvector and azimuth uncertainties, in nanostrain yr^{-1} .

varying crustal and constant total thicknesses overlying an inviscid asthenosphere; isostatic compensation of the crust is also assumed. This model is a reliable predictor of the horizontal components of velocity field, obtained by numerical integration of equations for the momentum balance, once the crustal thickness, the rheology and the boundary conditions are specified. The crustal thickness variation used in the analysis is obtained by linear interpolation onto the adopted grid of model CRUST 2.0 (Bassin *et al.* 2000; <http://mahi.ucsd.edu/Gabi/rem.html>). The domain is discretized using planar finite triangular elements sufficiently small in size (no bigger than $1^\circ \times 1^\circ$ in Central and Northern Europe, Fig. 5, and $2^\circ \times 2^\circ$ in the western oceanic portion of the domain) to justify treating the surface of each individual grid element as flat. The finite element modelling allows us to treat lateral variations in the viscosity. In this modelling aspect, the present comparative analysis takes, as its starting point, the major conclusions obtained by Marotta *et al.* (2004) and Marotta (2005), in the framework of a large-scale comparative analysis between predicted and geodetic deformation in Central and Northern Europe.

Their final statistical analysis indicates that the models that best fit the geodetically retrieved large-scale deformation in Central and Northern Europe include two major horizontal rheological heterogeneities, the Eastern European platform and the Mediterranean domain, differing for at least two order of magnitude in their effective viscosity. For what concerns the velocity boundary conditions, the second major constituent of the finite element tectonic model, to enlighten the impact that a different choice of velocity boundary conditions has on the results of a predicting model, three major sets of models have been implemented, which differ in terms of the Africa–Eurasia convergence velocity. *NU* model accounts for an Africa–Eurasia convergence constrained by the global plate motion model NUVEL-1A; *DE* model accounts for an Africa–Eurasia convergence constrained by the geodetic Deos-2k solution. Since Africa–Eurasia rotation pole indicated by Deos2k is different from



Figure 5. Cartoon showing the geometry, dimension and boundary conditions of the geophysical model. The Southern border of the model domain is chosen to coincide with the location of the Africa–Eurasia plate contact, taken from the ‘PLATES Project digital data compilation’ (<http://www.ig.utexas.edu/research/projects/plates/>). To prevent the figure from being too busy, only two portions of the numerical grid have been drawn inside the modelled domain. For further details, refer to the text.

that indicated by ITRF2005, to make predicted velocities, and thus predicted deformation totally consistent with geodetic velocities solutions of ITRF2005, another set of models (*IT* model) have been implemented in which the Africa–Eurasia boundary conditions are based on the ITRF2005 velocities. The new boundary conditions along the southern border of the model in the present analysis represent a major advancement with respect to Marotta *et al.* (2004) since the present definition of the Africa–Eurasia relative motion along the Southern border of the finite element model is not based solely on geological data through the NUVEL-1A plate motions model but also on appropriate GPS data that, with respect to previous work, allow us to define the Africa–Eurasia relative motion at a higher accuracy. By comparing the predictions of the different models, we are now able to quantify, at least for the study area, the misfit between modelling predictions and data and to discuss how much of it can be related to inappropriate choices of boundary constraints.

Fig. 6(a) shows the velocity boundary conditions applied at the southern boundary of the model—from NUVEL-1A, grey arrows, from Deos-2k, black arrows and from ITRF2005, white arrows—evaluated at the nodes of the finite element mesh defining our model. All, NUVEL-1A, Deos-2k and ITRF2005, indicate a counter-clockwise rotation of Africa with respect to Eurasia. Compared with NUVEL-1A, the GPS based Deos-2k and ITRF2005 indicate a smaller magnitude of the velocities, with the maximum variation of about 50 per cent, occurring south of the Calabrian arc (Fig. 6b). A significant variation in the azimuth to the west is also evident, which is almost constant at about 7 per cent along the southern border of the Tyrrhenian basin, decreasing to the west (Fig. 6c). It is important to note that the two GPS based boundary conditions portray minor differences in the Central Mediterranean, the object of our study, whereas they portray some deviations in the western

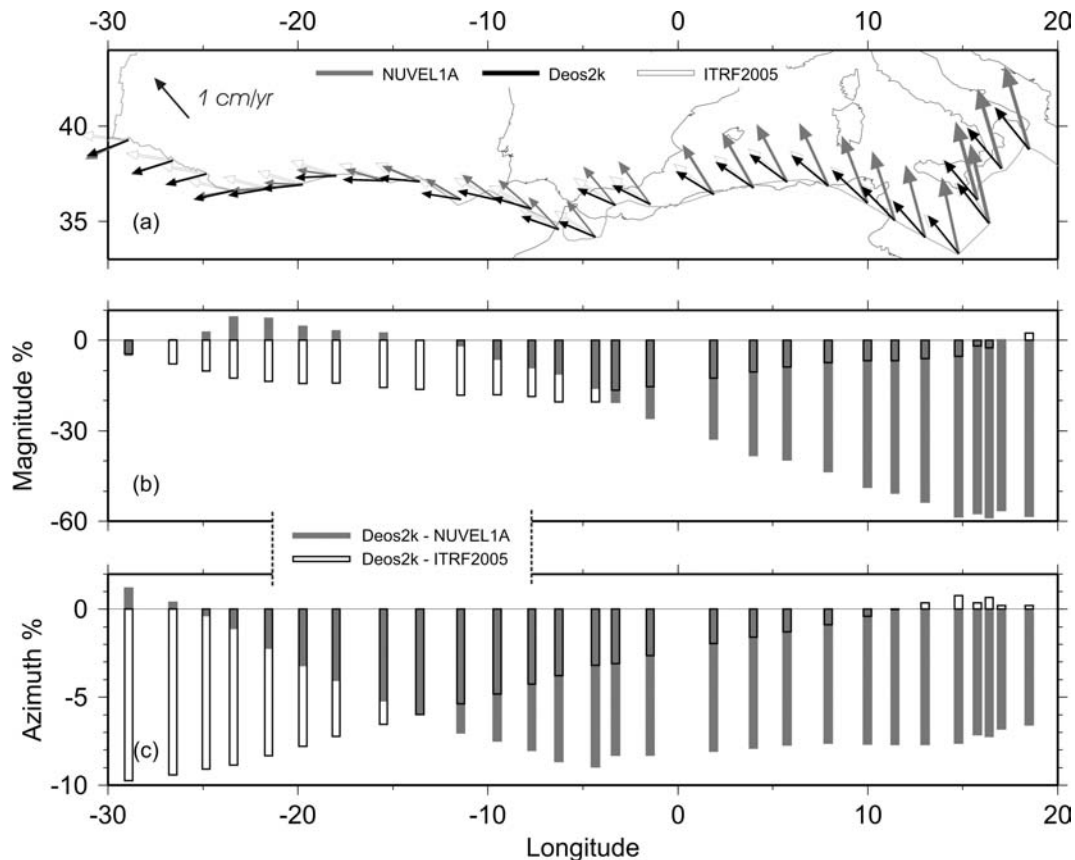


Figure 6. (a) Velocity boundary conditions applied at the southern boundary of the model—from NUVEL-1A, grey arrows; from Deos-2k, black arrows and ITRF2005, empty arrows—evaluated at the nodes of the finite element mesh defining our model. (b) Variation (in per cent) in the magnitude of Deos-2k solution with respect to NUVEL 1A (grey colour rectangles) and ITRF2005 (black contoured empty rectangles), as function of longitude. (c) Variation (in per cent) in the azimuth of Deos-2k solution with respect to NUVEL 1A (grey colour rectangles) and ITRF2005 (black contoured empty rectangles), as function of longitude.

Mediterranean, between Africa and the Iberian peninsula. It is relevant to analyse the effects of this newly derived GPS boundary conditions of Africa–Eurasia convergence on the tectonic model, thus, providing a realistic description of the deformation patterns in the Central Mediterranean, based on GPS based observable such as GPS derived baseline rates and strain rates, consistently compared with modelled ones driven by GPS derived Africa–Eurasia boundary conditions.

To minimize the boundary effects, the western border of the model domain is chosen to coincide with the location of the mid Atlantic Ridge (Fig. 5), where velocity boundary conditions vanish, in accordance with the concept that the effects of ridge push forces are completely absorbed between the ridge and the study domain (Marotta *et al.* 2004). The boundary conditions along the other model boundaries are the same as in Marotta *et al.* (2004).

4 RESULTS AND DISCUSSION

Fig. 7(a) shows the velocity field predicted in the Central Mediterranean by *NU* model. Three major domains can be distinguished. The first domain coincides with the area in proximity of the southern Africa–Eurasia border up to latitude of about 41° , where the velocity field is SE–NW directed, according to the Africa–Eurasia convergence, and the largest velocity gradients, both in magnitude and in direction, are located. The Central Tyrrhenian area, between 41° and

45° latitude, is characterized by velocities that are S–N directed and undergo a slow decrease, with contour lines roughly parallel to the Africa–Eurasia boundary, reaching 1 mm yr^{-1} in proximity of the Alpine front. At higher latitudes, deformation due to Africa–Eurasia convergence is further reduced and a small clockwise rotation of the velocities occurs. This effect is due to lithosphere weakening in the Mediterranean domain, as is evident by comparison with Fig. 7(b) where, north of the Alps, a NW trending velocity field, parallel to Africa–Eurasia convergence, is obtained from *NU* model, without softening of the Mediterranean domain.

Velocity field in Fig. 7 induces the deformation pattern shown in Fig. 8, where the colour map indicates the strain regime (red for compression and blue for extension) and the bars indicate the two eigenvectors of the strain rate, evaluated within each triangle of the numerical grid. Red indicates shortening and blue elongation; the length of the bars is proportional to the magnitude of the eigenvector, as shown by the colour scale. The study domain is marked by a diffuse compressional regime, reaching its largest intensity in the southern portion of the Adriatic area, whereas a soft extension occurs in proximity of the southern border of the model, where the most significant longitudinal variation in the velocity field is obtained. The almost total absence of longitudinal variation of the velocity field in the Central Tyrrhenian prevents the local development of any extension. Although very light, some extension appears again at high latitudes due to the clockwise rotation of the velocity field.

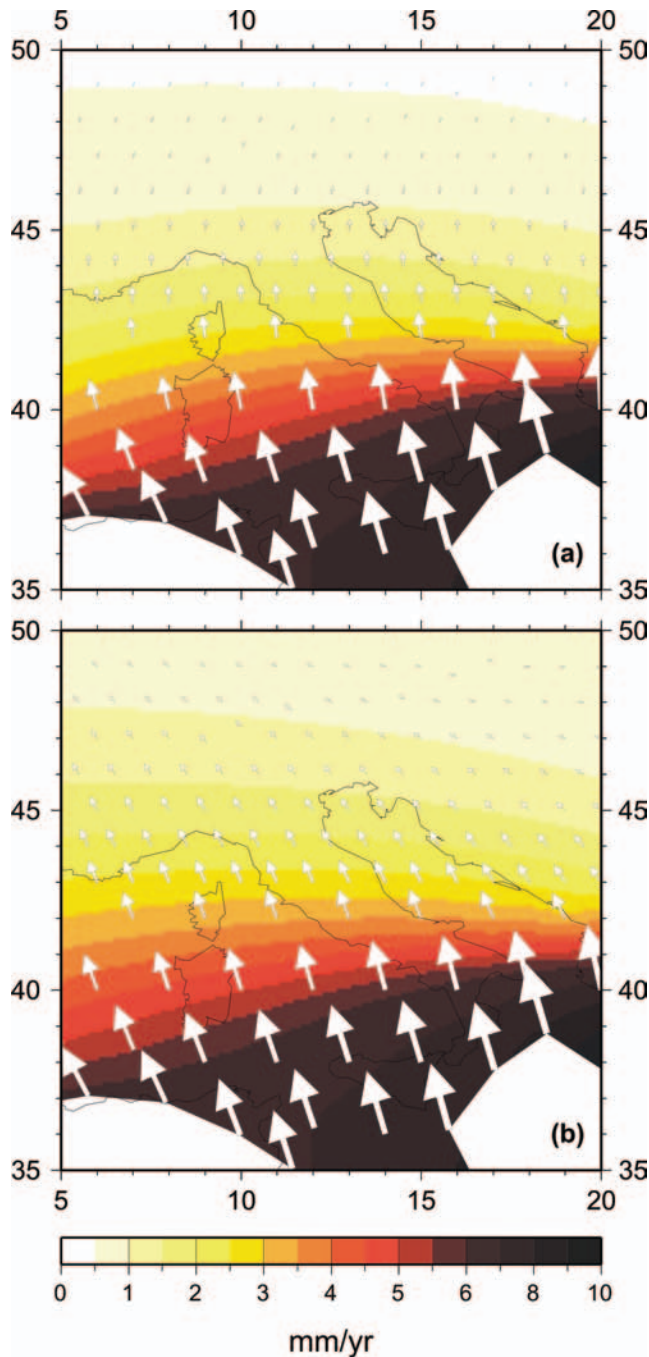


Figure 7. Velocity field (both arrows and colour) predicted in the Central Mediterranean by model *NU* (panel a) in which the velocity boundary conditions applied at the Southern boundary of the model are derived from NUVEL-1A and the rheological stratification accounts for both a stiff Baltic shield and a soft Mediterranean domain. Panel (b) shows the same as in panel (a) but obtained from model *NU*, without softening of the Mediterranean domain.

Fig. 9 compares the baseline rates predicted by *NU* model with the baseline rates obtained from ITRF2005 (yellow for shortening and cyan for elongation) shown in Fig. 2; red indicates predicted shortening and blue predicted elongation. Agreement between predictions and data is poor. In fact, although along almost all baselines the predicted deformation has the same style as indicated by the data (e.g. CAGL–LAMP, CAGL–NOTO, GENO–NOTO, VENE–

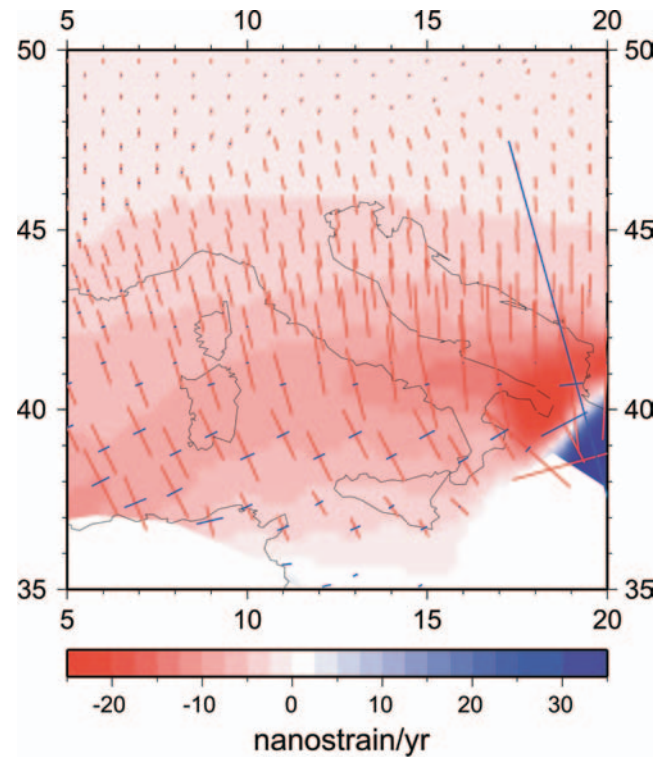


Figure 8. Strain regime (colour map, with red for compression and blue for extension) predicted in the Central Mediterranean by model *NU*. Bars indicate the two eigenvectors of the strain rate, evaluated within each triangle of the numerical grid. Red indicates the compressive component, whereas blue indicates the extensional one. The length of the bars is proportional to the magnitude of the eigenvector.

NOTO, VENE–MATE GENO–CAGL, VENE–GRAZ, OBER–VENE and GRAZ–MATE baselines shorten; CAGL–MATE and GENO–OBER baselines undergo elongation), three major elements shed doubts on the correctness of the model hypotheses. First, along some of the principal baselines (GENO–NOTO, VENE–NOTO and VENE–MATE), *NU* notably overestimates shortening, by as much as 200 per cent of the geodetic values. Second, in contrast to geodetic data, *NU* model does not predict any deformation along baseline NOTO–LAMP in the south. Finally, along the VENE–CAGL, VENE–GENO, OBER–GRAZ and NOTO–MATE baselines, shortening is predicted instead of elongation.

This discrepancy between model prediction and geodetic data is evident also in the 2-D deformation pattern. Fig. 10 compares the triangular strain rate eigenvectors predicted by *NU* model (red bars for compression and blue bars for extension) against the geodetic triangular strain rate eigenvectors shown in panel b of Fig. 3. Modelling decidedly overestimates the compressive component of the triangular strain rate in the GENO–CAGL–VENE, CAGL–MATE–VENE and VENE–MATE–GRAZ triangles; for the other triangles, both compression and extension is underestimated. However, the most important discrepancy between model and data is found in most of the eigenvector directions, which are well above the uncertainty intervals.

When Deos-2k geodetic solutions are used to force the model along the Southern border, significant modifications are induced on the regional deformation pattern, as shown in Fig. 11(a). First of all, due to the average 50 per cent decrease in the magnitude of the Africa–Eurasia relative velocity (Fig. 6), a less intense velocity field is predicted at low latitudes by *DE* model. This difference in

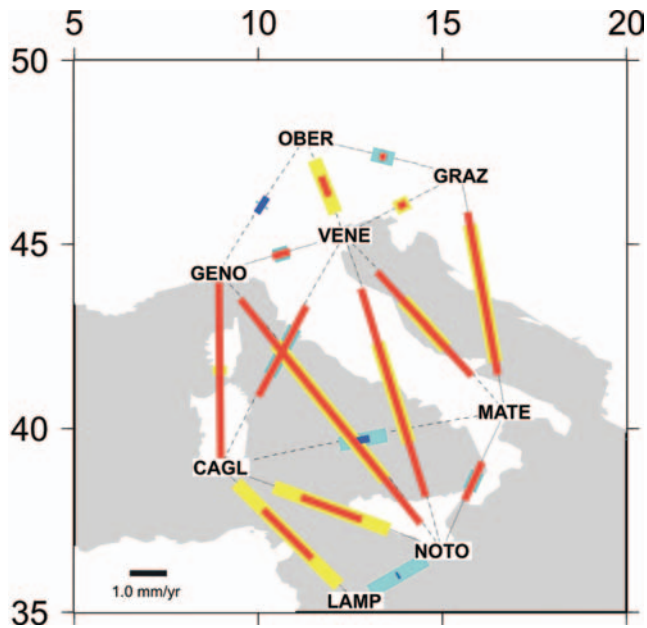


Figure 9. Baseline rates predicted by model *NU*, compared with the baseline rates obtained from ITRF2005 and shown in Fig. 2 (yellow for shortening and cyan for elongation). Red indicates predicted shortening whereas blue indicates predicted elongation.

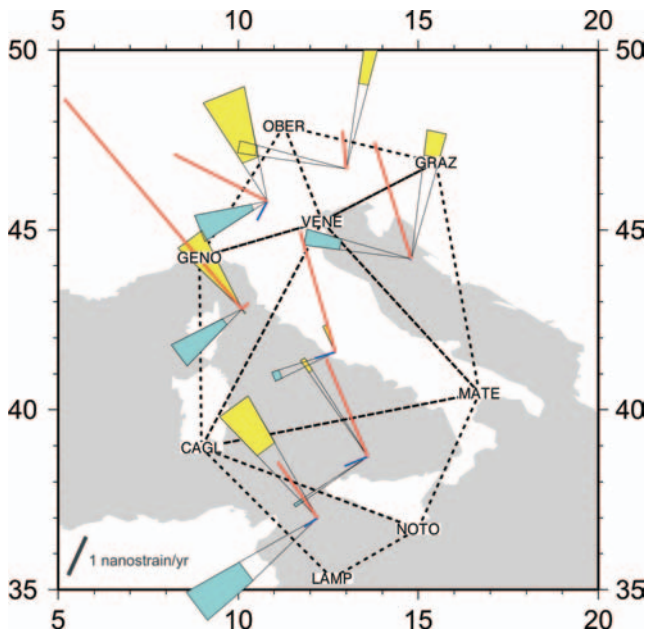


Figure 10. Triangular strain rate eigenvectors predicted by model *NU* (red bars for compression and blue bars for extension), compared with the geodetic triangular strain rate eigenvectors shown in Fig. 3(b).

magnitude decreases when we move to higher latitudes. However, the features that modify the deformation pattern the most are the large counter-clockwise rotation in the orientation of the velocity field at low latitudes, due to the increase of the counter-clockwise rotation of Africa with respect to Eurasia, and the less intense clockwise rotation of the velocity pattern at high latitudes, with respect to the velocity field forced by NUVEL-1A portrayed in Fig. 7(a).

As expected, in proximity of the southern border of the Tyrrhenian sea, the velocity field predicted by the model constrained by

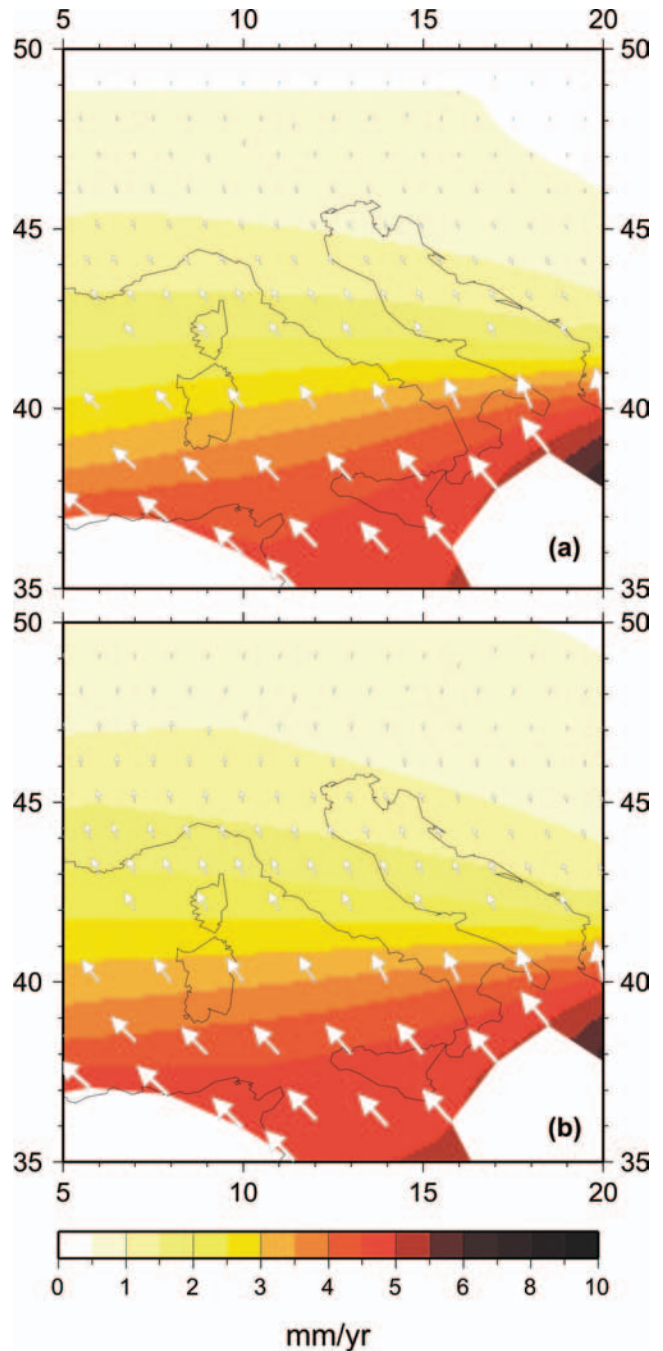


Figure 11. Velocity field (both arrows and colour) predicted in the Central Mediterranean by model *DE* (panel a) and model *IT* (panel b).

the boundary condition deduced from ITRF2005 (Fig. 11b), does not significantly deviate from that predicted by model constrained by Deos2k geodetic solution, and appreciable differences can be detected only at longer wavelengths, where a more intense extrusion to the east occurs.

Fig. 12 shows the strain rate fields associated with the velocity fields of Fig. 11. With respect to the results of the model based on NUVEL-1A, both new models predict a more intense extensional component of the strain rate tensor all around the Central Mediterranean, in the SW–NE direction, whereas the prevalent SE–NW compression decreases, thus, allowing the development of an extensive regime in a wider area compared with *NU* model of Fig. 8.

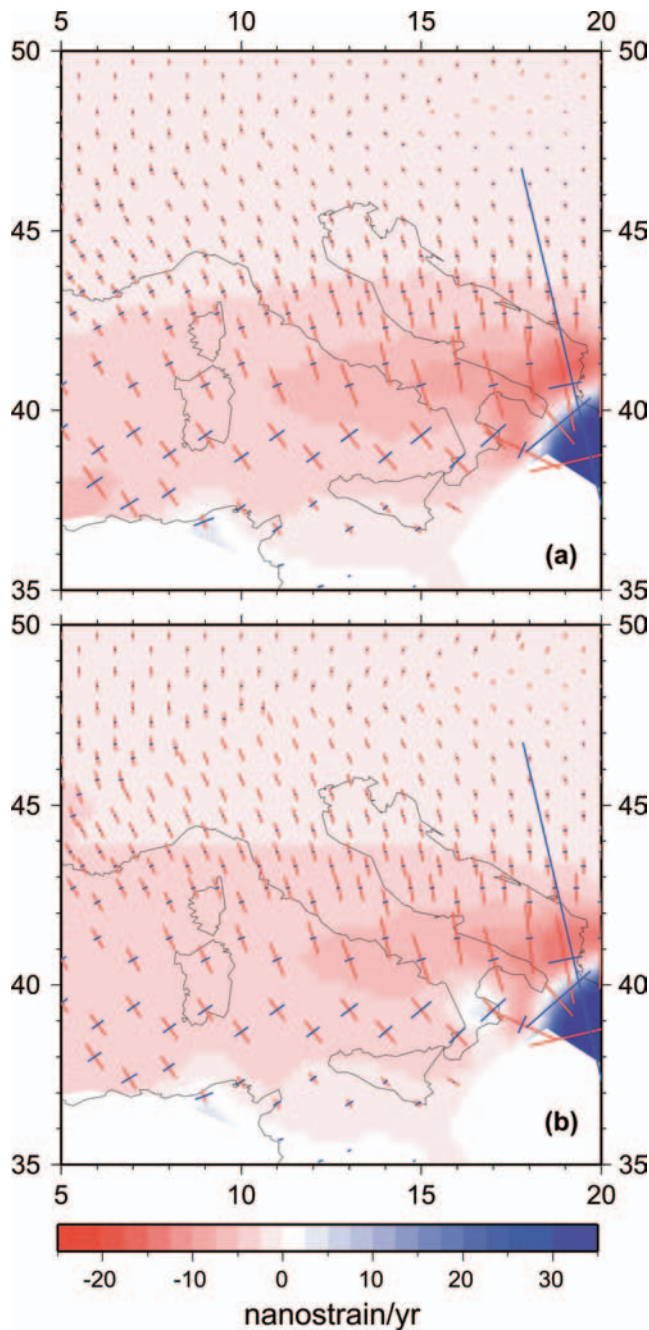


Figure 12. Strain regime (colour map, with red for compression and blue for extension) predicted in the Central Mediterranean by model *DE* (panel a) and model *IT* (panel b). Bars indicate the two eigenvectors of the strain rate, evaluated within each triangle of the numerical grid. Red indicates the compressive component, whereas blue indicates the extensional one. The length of the bars is proportional to the magnitude of the eigenvector.

In particular, *IT* model enhances the development of an extensional focus centred in the Calabrian area (Fig. 12b).

Fig. 13 compares the baseline rates predicted by *DE* (panel a) and *IT* (panel b) models to the baseline rates obtained from ITRF2005 (yellow for shortening and cyan for elongation), shown in Fig. 2. The improvement introduced by model *DE* is evident in two major aspects. First, along almost all the considered baselines, the predicted deformation has the same style as indicated by the data, with a now predicted S–N directed compression and an E–W directed

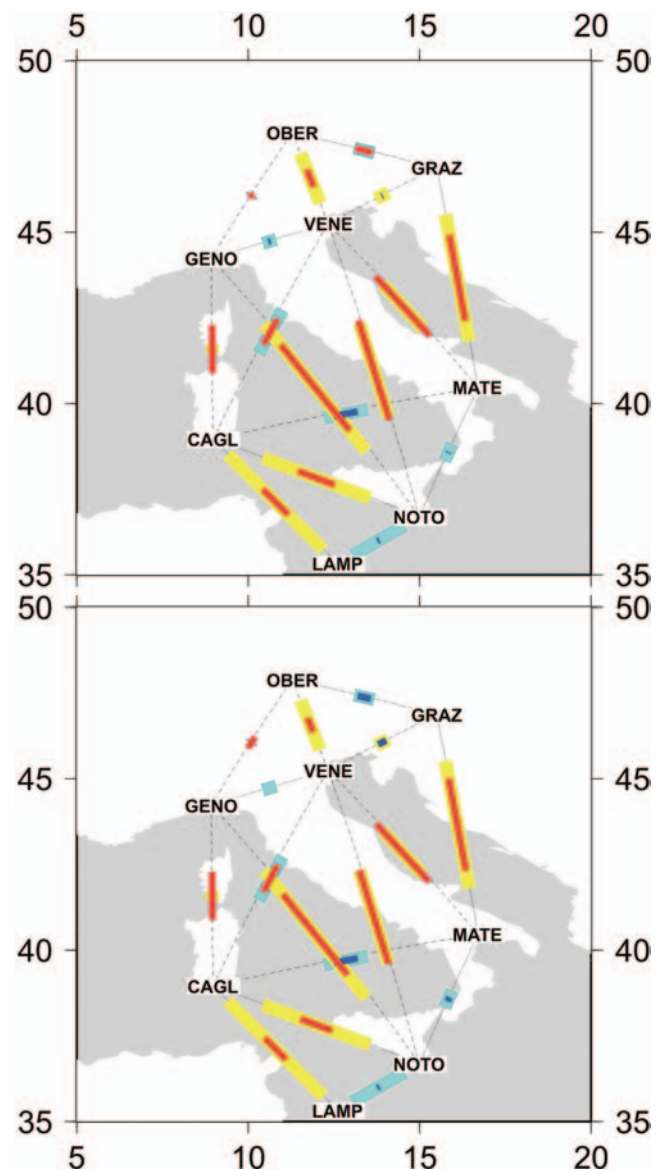


Figure 13. Baseline rates predicted by model *DE* and model *IT* (panel b), compared with the baseline rates obtained from ITRF2005 and shown in Fig. 2 (yellow for shortening and cyan for elongation). Red indicates predicted shortening while blue indicates predicted elongation.

extension, except for OBER–GRAZ along which, in contrast to geodetic data, *DE* model predicts shortening instead of elongation, GRAZ–VENE along which no significant deformation is predicted, as occurs for *NU* model, and OBER–GENO along which the observed extension is in any case small. The misfit along CAGL–VENE baseline, although persisting, is substantially reduced. The magnitude of the baseline rates predicted by this model is significantly reduced compared with *NU* model, improving the fit with the baselines subjected to shortening with respect to *NU*. It is notable that, in agreement with geodetic data and in distinct contrast with Fig. 9 where shortening is predicted, MATE–NOTO baseline now undergoes extension, although barely visible. Extension is also substantially increased with respect to Fig. 9 along the CAGL–MATE baseline, crossing the whole Tyrrhenian and Apennines. *IT* model further improves the fit between predicted and observed deformation in the west–east direction, as evident along NOTO–MATE

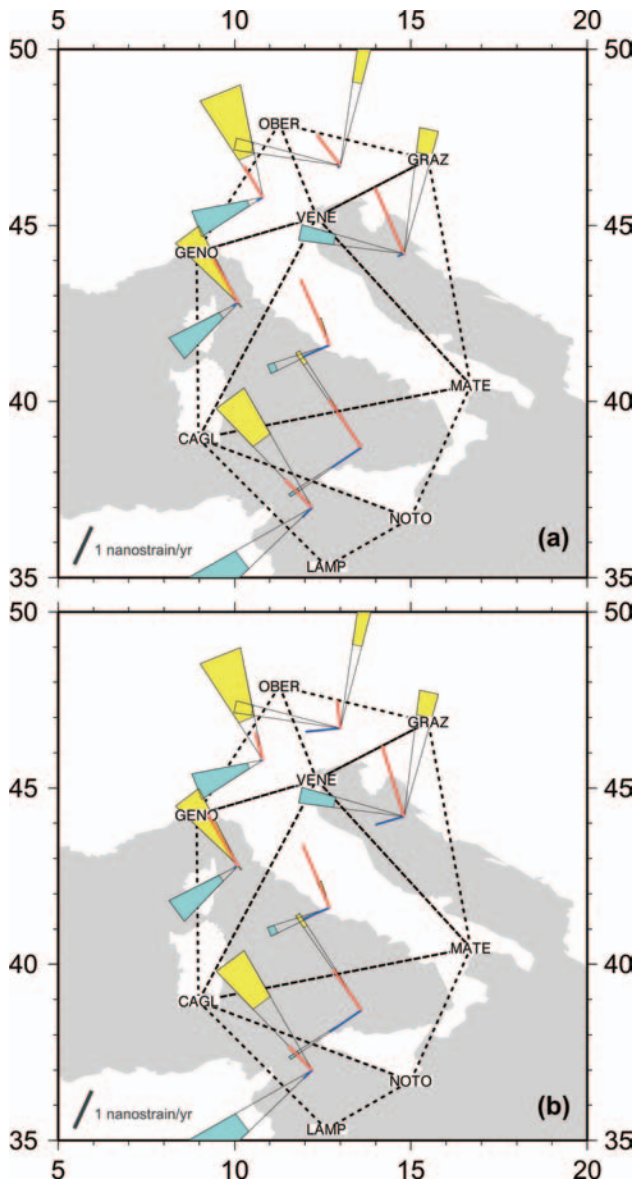


Figure 14. Triangular strain rate eigenvectors predicted by model *DE* (panel a) and model *IT* (panel b), red bars for compression and blue bars for extension, compared with the geodetic triangular strain rate eigenvectors shown in Fig. 3(b).

baseline, where extension is increased, and along OBER–GRAZ baseline, where, different from *NU* and *DE* models, extension is predicted, in agreement with geodetic data. This last result confirms that, when applied to the Mediterranean area, predictive models constrained through ITRF2005 solutions are more suitable to reproduce observed deformation at higher distances from the convergence boundaries.

The good fit between model prediction and geodetic data is evident also in the 2-D deformation pattern, portrayed in Fig. 14. Although *DE* and *IT* models still generally underestimate the magnitude of the deformation within the errors bounds, the direction of both compressive and extensive components of the predicted triangular strain rates is in complete agreement with the geodetic triangular strain rates in the Tyrrhenian area. Only within the triangles OBER–GRAZ–VENE and VENE–MATE–GRAZ, east of the Apennines chain, does *DE* model, like *NU* model, fail to repro-

duce the direction of the strain rate eigenvectors. This failure is, at least partly, overcome by *IT* model that, beyond predicting compression of comparable magnitude to that predicted by *DE* model, does predict a significant extensional component of deformation in the SW–NE direction, in agreement with observation, although not totally aligned with it (Fig. 14b).

To better assess the role of viscosity heterogeneities across the Mediterranean in the regional strain pattern and how much of the observed extension can be ascribed to the lateral inhomogeneities, we implement a series of numerical models in which the Adria microplate is a rheologically separate block in the geodynamic complex of the Mediterranean. The extension and tectonics of the Adria microplate are still debated and several models have been proposed: Adria as a region of a diffuse deformation within the entire Mediterranean region (e.g. Nocquet *et al.* 2001); Adria as part of Nubia (e.g. Mele 2001); Adria as a single block, independent from both Nubia and Eurasia (e.g. Anderson & Jackson 1987) and Adria subdivided into two separate blocks (e.g. Oldow *et al.* 2002). Recent geodetic analysis validate the independent identity of the Adria microplate, although they cannot discriminate between a single and a two block Adria subdivision (e.g. Battaglia *et al.* 2004), as it is supported by geological and geophysical observations (e.g. Calcagnile & Panza 1981; Venisti *et al.* 2005). In our models, the Adria microplate extends from the Po Valley, through the Adriatic Sea and Apulia, and it is delimited by the Kefallinia fault to the south and is subdivided into two blocks along the Gargano-Dubrovnik fault (Fig. 15). Different rheological contrasts between these blocks and the reference Mediterranean domain have been tested.

Fig. 16 focuses on the effects of lateral viscosity variations within the Adria plate with respect to the surrounding and includes the subdivision of this plate into two blocks, with the southern block stiffer by one order of magnitude than the northern one, Figs 16(a) and (b), models Reo-1 and Reo-2, respectively, compared with a uniform viscosity Adria microplate in Fig. 16(c), model Reo-3. In Fig. 16(a), the southern part of Adria is as stiff as the European plate, whereas in Fig. 16(b), it is one order of magnitude stiffer than

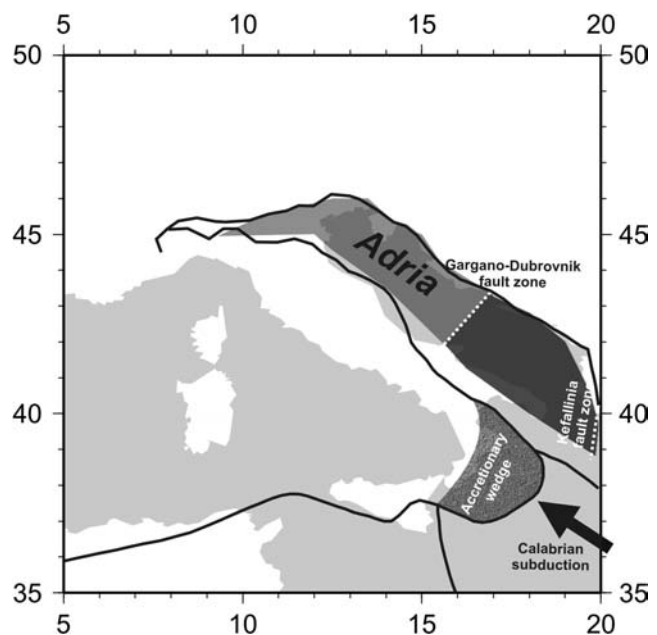


Figure 15. Cartoon showing the geometry of the two blocks constituting the Adria microplate and the setup of the Calabrian subduction, as assumed within this study.

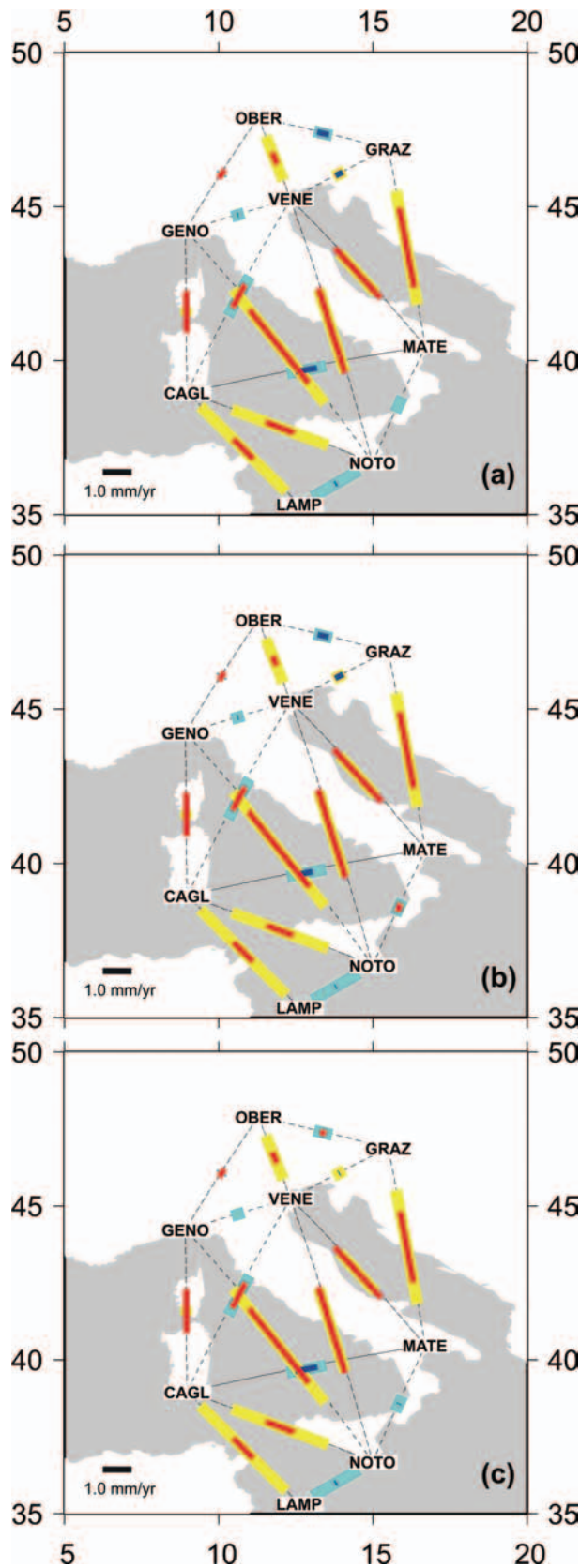


Figure 16. Baseline rates predicted by models Reo1 (panel a), Reo2 (panel b) and Reo3 (panel c), compared with the baseline rates obtained from ITRF2005 and shown in Fig. 2 (yellow for shortening and cyan for elongation). Red indicates predicted shortening whereas blue indicates predicted elongation.

the latter. Once compared with Fig. 13(b), we note that the stiffening of the Adria plate with respect to the Mediterranean domain has the effect to improve the fit of the data along the GENO–VENE baseline where, now, extension appears in agreement with the observational data, and to slightly decrease shortening along the SE–NW directed baselines; Adria plate stiffening degrades the fit along the NOTO–MATE baseline, where extension disappears now. A viscosity increase by one order of magnitude in both parts of the Adria plate (Fig. 16b) is responsible for a further degradation of the fit along this NOTO–MATE baseline, by inverting the style of deformation, which is now shortening rather than extension. A uniform viscosity increase in the whole Adria plate (Fig. 16c) by one order of magnitude with respect to the Mediterranean, improves the NOTO–MATE baseline deformation style with respect to Fig. 16(b), by allowing for the re-appearance of the extension, although of limited intensity. This improvement is counteracted by the inversion of the deformation style in the north, where OBER–GRAZ now portrays shortening rather than extension. Lateral viscosity variations in the central Mediterranean, associated with that expected for the well established presence of the Adria plate, does not seem to produce any improvement with respect to the uniform viscosity model.

The underestimation of the W–E extension could be partially ascribed to the lack of allowance for subduction into the thin sheet model. In particular, part of the S–N shortening, due to Africa–Eurasia convergence, could be absorbed into the Calabrian subduction. The inclusion of subduction into a thin sheet model is not trivial. We tried two different approaches. In the first attempt, we simply define the accretionary wedge, associated with Calabrian subduction, through a set of extremely weak element. However, this approach did not reveal to be successful, and strain rate pattern resulted was essentially unaffected, even for values of the effective viscosity in the accretionary wedge less by three orders of magnitude than the surroundings. In the second approach, we specify progressively decreasing convergence velocities at the nodes of the numerical grid delimiting the Calabrian trench. In the following, we will discuss results of the models in which reduced convergence velocities along the Calabria subduction act in concert with the lateral viscosity variations of the Adria microplate, discussed previously.

Figs 17(a) and (b) stand for the cases in which the 75 per cent of the convergence velocity is transmitted to the Eurasian plate through the Calabria subduction zone (models Reo1-0.75 and Reo3-0.75, respectively), whereas in Fig. 17(c), only the 50 per cent of the ITRF2005 convergence velocity is transmitted (model Reo1-0.5). To enlighten the effects of wedge absorption, Figs 17(a) and (b) of this figure must be compared with Fig. 16(a) and (c). In Fig. 17(a), extension along NOTO and MATE is now larger once compared with Fig. 16(a), and this important feature of the deformation pattern in central Mediterranean is now improved with respect to the homogeneous model of Fig. 13(b). With respect to both Figs 16 and 13, extension is increased also along the CAGL–MATE baseline. Absorption of 1/4 of the convergence velocity within the wedge, has thus the effects to increase extension along the E–W oriented baseline in the south, meanwhile maintaining shortening along the SE–NW baselines, in good agreement with observational data. Although Fig. 17(b) improves the extension with respect to the same uniformly viscosity stiffening of the Adria plate of Fig. 16(c), it does not overcome the shortcoming of this model along the OBER–GRAZ in the north, where shortening is predicted again rather than extension. This shortcoming is corrected in Fig. 17(c), where the 50 per cent of the convergence velocity is absorbed within the wedge, increasing the extension in the south, which is now in complete agreement with observational data. Shortening along the

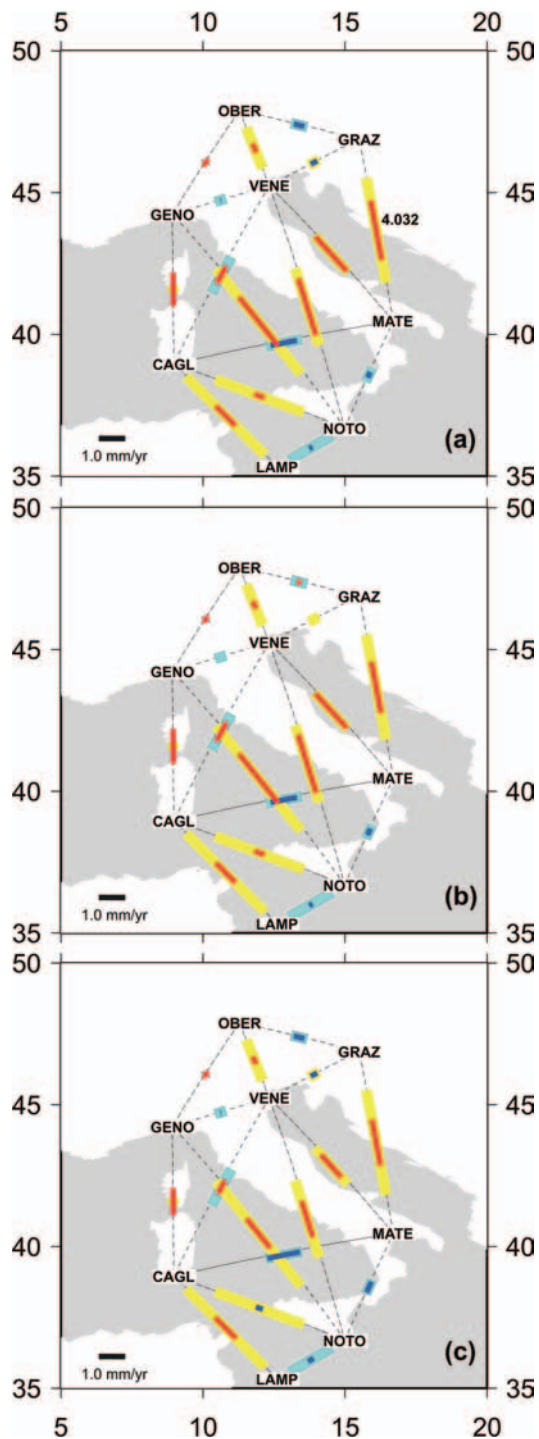


Figure 17. Baseline rates predicted by models Reo1-0.75 (panel a), Reo3-0.75 (panel b) and Reo1-0.5 (panel c), compared to the baseline rates obtained from ITRF2005 and shown in Fig. 2 (yellow for shortening and cyan for elongation). Red indicates predicted shortening while blue indicates predicted elongation.

SE–NW oriented baselines crossing the whole central Mediterranean is now reduced, actually inverting the deformation style along the CAGL–NOTO baseline, now turning into extension rather than shortening, as required by the data.

Model Reo1-0.75 has the effect to widen the area subjected to a dominant extension, with eigenvectors roughly perpendicular the

Italian peninsula (compare Fig. 18a with Fig. 12b). Extension now affects the whole southernmost part of Italy and easternmost part of the Tyrrhenian sea, between 15° and 17° longitude.

With model Reo1-0.5 this extensional area is further enlarged (Fig. 18b), now affecting the whole southern Tyrrhenian from about 10° longitude eastward. Besides the widening of the area under extension, we also note a reduction of the compressional eigenvalue,

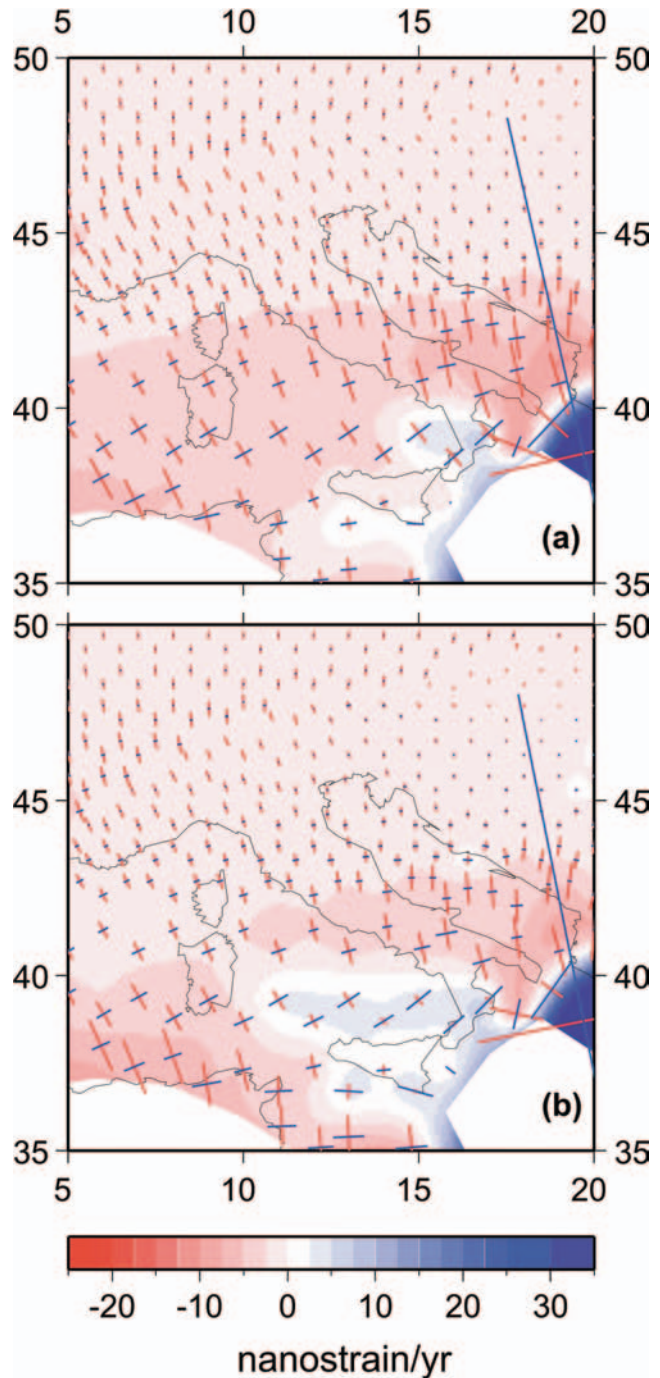


Figure 18. Strain regime (colour map, with red for compression and blue for extension) predicted in the Central Mediterranean by models Reo1-0.75 (panel a) and Reo1-0.5 (panel b). Bars indicate the two eigenvectors of the strain rate, evaluated within each triangle of the numerical grid. Red indicates the compressive component, whereas blue indicates the extensional one. The length of the bars is proportional to the magnitude of the eigenvector.

as indicated by the shorter red bars of Fig. 18(b) with respect to Fig. 18(a) within the blue area under dominant extension.

5 CONCLUSIONS

The new motion of Africa and Eurasia, as given by the Deos-2k plate motion model by Fernandez *et al.* (2003) and ITRF2005, improves the fit between the N–NW directed compression and the W–SW directed extension between Sardinia and Adriatic sites from ITRF2005, thanks to the combined effect of reduced amplitude of Africa–Eurasia relative velocity, which reduces the compression, and an increase in the westerly directed component with respect to NUVEL-1A, which increases the extension.

Overall, we obtain a good agreement in terms of eigendirections, especially west of the Adriatic sea or west of the baseline connecting Venice (VENE) and Matera (MATE), with degrading fit in terms of eigenvalue magnitudes, east of this line. For the longest baselines and, in particular, for the shortening ones covering the whole Italian peninsula or Southern Italy with eastern Europe, changes are of the order of few millimeters at most, which makes strain-rates, at the global scale, of the order of some nanostrains yr^{-1} . Our results are thus indicative of the deformation style at the regional, or global, scale but certainly cannot be used to estimate strain-rates in specific, highly deforming seismogenic zones, where faults or large lateral effective viscosity variations occurring at the very short wavelength, can be important.

This comparative study shows that within the study area the velocity field, strain rate, baseline rate and triangular strain rate, based on ITRF2005 boundary conditions, deviate from those based on Deos2k only at long distances from the Africa–Eurasia boundary. This is in agreement with Devoti *et al.* (2008) who show that, although based on different reference systems, different data set and different assumptions, the relative angular velocity poles of Africa with respect to Eurasia for ITRF2000 (on which Deos2k is based) is consistent (within their sigma) with that derived for ITRF2005, and that the small differences are not statistically significant.

Cross-check of geodetic and geophysical model deformation patterns, thus, proves to be of fundamental importance for validating realistic finite element tectonic models and to verify the effects of active tectonics within the highly deforming Mediterranean embedded within the Africa–Eurasia collision zone.

ACKNOWLEDGMENTS

AMM was funded by the Italian Ministry of Universities and Research (M.I.U.R.) under the project entitled ‘Strain and Stress analysis in the Central European Basin System: integration of numerical modelling with geological, geophysical and satellite data.’ (COFIN 2005). RS was funded by the Italian Space Agency project ‘Seismic Information System for Monitoring and Alert’ (SISMA). The authors acknowledge Rui Fernandez for providing the boundary conditions along the Africa–Eurasia boundary of our numerical model, based on Deos2k velocity solutions, and Roberto Devoti for providing the boundary conditions along the Africa–Eurasia boundary of our numerical model, based on ITRF2005 velocity solutions. Authors thank the Editor and two anonymous reviewers for their constructive criticisms. All figures were created using GMT plotting software (Wessel & Smith 2001).

REFERENCES

- Altamini, Z., Sillard, P. & Boucher, C., 2002. ITRF2000: a new release of the International Terrestrial Reference Frame for Earth science applications, *J. geophys. Res.*, **107**, doi:10.1029/2001B000561.
- Altamini, Z., Collilieux, X., Legrand, J., Garayt, B. & Boucher, C., 2007. ITRF2005: a new release of the International Terrestrial Reference Frame on the time series of station positions and Earth orientation parameters, *J. geophys. Res.*, **112**, doi:10.1029/2007JB004949.
- Anderson, H. & Jackson, J., 1987. Active tectonics of the Adriatic region, *Gephys. J. Int.*, **91**, 937–983.
- Bassin, C., Laske, G. & Masters, G., 2000. The current limits of resolution for surface wave tomography in North America, *EOS, Trans. Am. geophys. Un.*, **81**, F897.
- Battaglia, M., Murray, M.H., Serpelloni, E. & Burgmann, R., 2004. The Adriatic region: an independent microplate within the Africa–Eurasia collision zone, *Geophys. Res. Lett.*, **31**, doi:10.1029/2004GL019723.
- Calcagnile, G. & Panza, G.F., 1981. The main characteristics of the lithosphere–asthenosphere system in Italy and surrounding regions, *Pure appl. Geophys.*, **119**, 865–880.
- CRUST 2.0. Available at <http://mahi.ucsd.edu/Gabi/rem.html>.
- DeMets, C. & Dixon, T.H., 1999. New kinematic models for Pacific–North America motion from 3 Ma to present; I. Evidence for steady motion and biases in the NUVEL-1A model, *Geophys. Res. Lett.*, **26**, 1921–1924.
- DeMets, C., Gordon, R.G., Argus, D.F. & Stein, S., 1994. Effect of recent revisions to the geomagnetic reversal timescale on estimates of current plate motions, *Geophys. Res. Lett.*, **21**, 2191–2194.
- Devoti, R., Riguzzi, F., Cuffaro, M. & Doglioni, C., 2008. New GPS constraints on the Apennine subduction, *Earth planet. Sci. Lett.*, doi:10.1016/j.epsl.2008.06.031.
- Fernandez, R.M.S., Ambrosius, B.A.C., Noomen, R., Bastos, L., Wortel, M.J.R., Spakman, W. & Govers, R., 2003. The relative motion between Africa and Eurasia as derived from ITRF2000 and GPS data, *Geophys. Res. Lett.*, **30**, 1828, doi:10.1029/2003GL017089.
- ITRF2000, available at <http://lareg.ensg.ign.fr/ITRF/ITRF2000>.
- ITRF2005, available at http://lareg.ensg.ign.fr/ITRF_solutions/2005/ITRF2005.php.
- Jimenez-Munt, I., Sabadini, R., Gardi, A. & Bianco, G., 2003. Active deformation in the Mediterranean from Gibraltar to Anatolia inferred from numerical modeling, geodetic and seismological data, *J. geophys. Res.*, **108**(B1), doi:10.1029/2001JB001544.
- Kremer, C., Holt, W.E. & Haines, A.J., 2003. An integrated global model of present-day plate motions and plate boundary deformation, *Geophys. J. Int.*, **154**, 8–34.
- Marotta, A.M., 2005. The fingerprints of intra-continental deformation in Central Europe as envisaged by the synergic use of predicting modeling and geodetic data, *Bollettino di Geofisica Teorica ed Applicata*, **46**, 181–199.
- Marotta, A.M. & Sabadini, R., 2004. The signature of tectonics and glacial isostatic adjustment revealed by the strain rate in Europe, *Geophys. J. Int.*, **157**, 865–870.
- Marotta, A.M., Mitrovica, J.X., Sabadini, R. & Milne, G., 2004. Combined effects of tectonic and glacial isostatic adjustment on intraplate deformation in Central and Northern Europe: application to geodetic baseline analyses, *J. geophys. Res.*, **109**(B1), doi:10.1029/2002JB002337.
- Mele, G., 2001. The Adriatic lithosphere is a promontory of the African plate: evidence of a continuous mantle lid in the Ionian Sea from efficient Sn propagation, *Geophys. Res. Lett.*, **28**, 431–434.
- Negredo, A.M., Jimenez-Munt, I. & Villasenor, A., 2004. Evidence for eastward mantle flow beneath the Caribbean plate from neotectonic modeling, *Geophys. Res. Lett.*, **31**, doi:10.1029/2003GL019315.
- Nocquet, J.-M. & Calais, E., 2003. Crustal velocity field of western Europe from permanent GPS array solutions, 1996–2001, *Geophys. J. Int.*, **154**, 72–88.
- Nocquet, J.-M., Calais, E., Altamini, Z., Sillard, P. & Boucher, C., 2001. Intraplate deformation in western Europe deduced from an analysis of the International Terrestrial Reference Frame 1997 (ITRF97) velocity field, *J. geophys. Res.*, **106**, 11 239–11 257.

- Oldow, J.S. *et al.*, 2002. Active fragmentation of Adria, the north African promontory, central Mediterranean orogen, *Geology*, **30**, 779–782.
- Sella, F.G., Dixon, T.H. & Mao, A., 2002. REVEL: a model for recent plate velocities from space geodesy, *J. geophys. Res.*, **107**, doi:10.1029/2000JB000033.
- Topography and predicted bathymetry of the World with present-day plate boundaries, 1999. Available at <http://www.ig.utexas.edu/research/projects/plates>.
- Venisti, N., Calcagnile, G., Pontevivo, A. & Panza, G.F., 2005. Tomographic study of the Adriatic plate, *Pure appl. Geophys.*, **162**, 311–329.
- Wang, J. & Zheng-Ren, Y., 2006. Dynamic modeling for crustal deformation in China: comparisons between the theoretical prediction and the recent GPS data, *Phys. Earth planet. Inter.*, **155**, 201–207.
- Wessel, P. & Smith, W.M.F., 2001. New improved version of generic mapping tools released, *EOS, Trans. Am. geophys. Un.*, **79**, 579.